HHS Public Access

Author manuscript

*Nat Neurosci*. Author manuscript; available in PMC 2012 September 06.

Published in final edited form as:

*Nat Neurosci*. ; 15(2): 243–249. doi:10.1038/nn.3013.

# Uncoupling the roles of synaptotagmin I as a dual $Ca^{2+}$ sensor during endo- and exocytosis of synaptic vesicles

**Jun Yao**[*], **Sung E. Kwon**[*], **Jon D. Gaffaney**, **F. Mark Dunning**, and **Edwin R. Chapman**

Howard Hughes Medical Institute and Department of Neuroscience, University of Wisconsin, Madison, Wisconsin 53706

## Abstract

Synaptotagmin I (syt1) is required for normal rates of synaptic vesicle endo- and exocytosis. However, whether the kinetic defects observed during endocytosis in syt1 knock-out neurons are secondary to defective exocytosis, or whether syt1 directly regulates the rate of vesicle retrieval, remains unresolved. In order to address this question, it is necessary to dissociate these two activities. Here, we have uncoupled the function of syt1 in exo- and endocytosis by re-targeting of the protein, or via mutagenesis of its tandem C2-domains; the impact of these manipulations on exo- and endocytosis were analyzed via electrophysiology, in conjunction with optical imaging of the vesicle cycle. These experiments uncovered a direct role for syt1 in endocytosis. Surprisingly, either C2-domain of syt1 - C2A or C2B - was able to function as $Ca^{2+}$-sensor for endocytosis. Hence, syt1 functions as a dual $Ca^{2+}$ sensor for both endo- and exocytosis, potentially coupling these two limbs of the vesicle cycle.

## INTRODUCTION

Synaptic vesicle (SV) endo- and exocytosis are mediated by distinct ensembles of proteins that are somehow coordinated, or coupled, such that these two limbs of the vesicle cycle are kept in balance; this balance is critical to maintain releasable vesicle pools and to keep the area of the presynaptic plasma membrane relatively constant. One compelling candidate to link these two processes is synaptotagmin I (syt1), an integral membrane protein of SVs. A variety of studies - ranging from genetic analysis of syt1 mutants to reconstituted membrane fusion reactions - support the conclusion that syt1 functions as a major $Ca^{2+}$ sensor during SV exocytosis[1,2]. The cytoplasmic domain of syt1 harbors tandem C2-domains (C2A and C2B) that interact with $Ca^{2+}$, SNARE (soluble NSF attachment protein receptor) proteins and phospholipids to trigger membrane fusion. Furthermore, the C2B domain of syt1 was



Please address correspondence to: Edwin R. Chapman, Ph.D. 1300 University Avenue, 129 SMI, Madison, WI 53706; Telephone: (608) 263-5512; Fax: (608) 265-5512; chapman@physiology.wisc.edu.

[*]These authors contributed equally to the work done in this study.

F. M. Dunning's present address: BioSentinel Pharmaceuticals Inc., Madison, Wisconsin, 53719.

***AUTHOR CONTRIBUTIONS:*** J.Y., S.E.K., and E.R.C. designed the experiments. J.Y. conducted the electrophysiological and immunostaining experiments. S.E.K and J.Y. conducted pHluorin imaging experiments. F.M.D., S.E.K. and J.Y. conducted molecular biology experiments. J.D.G. conducted cell fractionation experiments. J.D.G. and J.Y. conducted immunoblot experiments. J.Y., S.E.K, and E.R.C. analyzed the data, and wrote the manuscript.

reported to bind to endocytic adaptor proteins (i.e. AP-2 and stonin-2), suggesting that syt1 may serve as a mediator of clathrin-dependent endocytosis[3–7]. Syt1 might therefore act to insure that the rates of endo- and exocytosis are balanced.

In accordance with this notion, imaging studies using electron microscopy, pH sensitive green fluorescent protein (pHluorin), or FM dyes have revealed endocytic defects in syt1-deficient synapses in a variety of organisms[8–10]. However, recent reports raise questions as to whether syt1 participates directly in endocytosis. For instance, mutations in the AP-2/stonin-2 binding motif of the C2B domain of syt1, or in the syt1 binding motif of stonin-2, do not affect the kinetics of SV endocytosis[7,11]. Moreover, loss-of-function mutations in syt1 that impair exocytosis generally result in defects in endocytosis (e.g. [11]), raising the question as to whether the apparent endocytic defects are in fact secondary to perturbation of vesicle fusion. Collectively, these results indicate that a definitive determination of whether syt1 directly regulates the rate of SV endocytosis requires the uncoupling of its function during endo- and exocytosis.

A parallel line of investigation has focused on $Ca^{2+}$, as changes in intracellular [$Ca^{2+}$] regulate both endo- as well as exocytosis. An effect of $Ca^{2+}$ on endocytosis has been confirmed at calyx of Held, hippocampal, and retinal bipolar cell synapses[15–18]. In the calyx of Held, $Ca^{2+}$ not only directly triggers endocytosis, but also modulates the kinetics of this process [13, 14]. However, in small central synapses, it appears that $Ca^{2+}$ only affects the macroscopic kinetics of SV endocytosis - but not the kinetics of unitary endocytic events - through increasing the capacity of the vesicle retrieval machinery[18].

In the current study, we uncoupled the function of syt1 during SV endo- and exocytosis and directly demonstrate a role for syt1 in endocytosis. Surprisingly, syt1 participates in $Ca^{2+}$ dependent vesicle retrieval through the $Ca^{2+}$ binding activity of either of its C2-domains. Moreover, we found that syt1 deletion mutants that harbored only a single C2-domain - C2A or C2B - were able to mediate the internalization of syt1. In summary, we conclude that in hippocampal neurons, syt1 functions as a dual $Ca^{2+}$ sensor during both endo- and exocytosis and can thereby help to couple these two processes to maintain balance within the SV cycle.

## RESULTS

### Effect of retargeted syt1 on SV endocytosis

We first investigated whether the defect in endocytosis observed in syt1 knock-out (KO) neurons can be directly attributed to the loss of syt1[8] or whether this defect is secondary to perturbation of exocytosis caused by the knock-out. One idea for how syt1 might regulate endocytosis is via the recruitment of adaptor proteins including AP-2 and stonin-2[3–7]. This model predicts that syt1 must be present at significant levels on nascent SVs in order to facilitate vesicle retrieval. To test this, we re-targeted the cytoplasmic domain of syt1 to the presynaptic plasma membrane (Fig. 1a). To achieve this, the cytoplasmic C2A-C2B domain of syt1 was fused to an N-terminal 20 amino acid segment of GAP-43, which is palmitoylated and anchored to the plasma membrane in neurons (Fig. 1b) and chromaffin cells (Supplementary Fig. 1) (see also [19]). In syt1 KO neurons, GAP43-C2AB was localized to presynaptic boutons, as revealed by co-staining with synapsin I (73 ± 5%, n = 6 images),

as was full-length wild type syt1 (syt1$^{FL}$: 79 ± 8%, n = 10 images) (Fig. 1c), but was expressed at a lower level than syt1$^{FL}$ (57%; Fig. 1d). To further investigate whether GAP43-C2AB was localized to SVs or the plasma membrane, we compared the distributions of syt1 and GAP43-C2AB by subcellular fractionation (Fig. 1e). Both native and exogenous syt1 were present in the SV and synaptosome fractions, with only low levels of GAP43-C2AB in the SV fraction (<4%).

To investigate the function of GAP43-C2AB in excitatory synaptic transmission, we compared evoked and miniature excitatory postsynaptic currents (EPSC) in syt1 KO neurons, and KO neurons infected with lentiviruses that express syt1$^{FL}$ or GAP43-C2AB (Fig. 1, Supplementary Fig. 2). Consistent with previous reports[20–22], single action potentials elicited relatively small asynchronous EPSCs in syt1 KO neurons (Fig. 1f, g; 138 ± 11 pA). In contrast, robust EPSCs were observed in neurons expressing syt1$^{FL}$ (781 ± 94 pA, $p<0.001$). GAP43-C2AB expression in syt1 KO neurons rescued evoked EPSCs with similar peak amplitudes as compared to syt1$^{FL}$ (818 ± 73 pA, $p>0.05$). Further analysis revealed similar kinetics of charge transfer during evoked transmission in neurons expressing syt1$^{FL}$ or GAP43-C2AB, which were much faster than for syt1 KO neurons (Fig. 1h); quantal size was similar in all three groups (Supplementary Fig. 2). GAP43-C2AB fully rescued the elevated miniature EPSC (mEPSC) frequency observed in syt1 KO neurons. Thus, plasma membrane-targeted syt1 restored normal spontaneous, as well as evoked, neurotransmitter release in syt1 KO neurons. As noted above, the proportion of GAP43-C2AB on SVs was low (Fig. 1e); we estimate that on average there will be less than one copy of GAP43-C2AB per SV.

Next, to directly monitor the effects of GAP43-C2AB on the SV cycle, we performed live-cell imaging of pHluorin tagged synaptophysin (sypHy)[23,24]. This reporter is efficiently quenched by low pH in the vesicle lumen and becomes bright upon exocytosis[25]. SypHy and GAP43-C2AB were expressed through double lentiviral infection (Fig. 2a), and exocytosis was evoked by applying a 20 Hz field stimulus for 5 s (Fig. 2b, c)[26,27]. We confirmed that syt1 KO hippocampal neurons exhibited slower rates of endocytosis, with a significantly longer time constant ($\tau$) ($\tau$ = 31.6 ± 0.6 s, $p<0.001$) as compared to wild-type (WT) neurons ($\tau$ = 18.2 ± 0.5 s) (Fig. 2b, d)[10]. The kinetic defects in endocytosis in KO neurons were fully rescued by expressing syt1$^{FL}$ ($\tau$ = 19.0 ± 0.6 s, $p>0.05$).

Notably, GAP43-C2AB was unable to rescue the slow rates of endocytosis observed in syt1 KO neurons (Fig. 2b, d; $\tau$ = 36.7 ± 0.4 s, $p<0.001$, compared to WT neurons). We note that the endocytic $\tau$ exhibited by syt1 KO neurons was slightly increased by GAP43-C2AB (Fig. 2d; $p<0.001$, compared to syt1 KO neurons). However, this appears to be a secondary effect resulting from the KO because over-expression of GAP43-C2AB in WT neurons had no effect on the rate of vesicle internalization (Fig. 2b, d; $\tau$ = 20.2 ± 0.7 s, $p>0.05$, compared to WT neurons). Because the shape of the fluorescence decay of syt1 KO neurons expressing GAP43-C2AB was not strictly mono-exponential (Fig. 2b), we also compared the 50% fluorescence decay time between samples (Fig. 2e) and similar trends were observed. We also performed FM4-64 uptake experiments to confirm that SV endocytosis was differentially affected by syt1$^{FL}$ versus GAP43-C2AB in syt1 KO neurons (Supplementary Fig. 3).

Together, the findings reported thus far suggest that in syt1 KO neurons, GAP43-C2AB was able to restore rapid SV exocytosis but failed to rescue defects in endocytosis. To our knowledge, this is the first example of uncoupling these two functions of syt1. While this uncoupling might be due to the retargeting of the C2AB-domain to the plasma membrane, we cannot exclude the possibility that the low levels of GAP43-C2AB on SVs (Fig. 1e) were sufficient to regulate normal rates of release but not normal rates of vesicle retrieval.

## Uncoupling syt1 in exo- and endocytosis via mutations

During exocytosis, the C2-domains of syt1 interact with $Ca^{2+}$, SNAREs, and lipids in the plasma membrane[2]. Recent studies indicate that $Ca^{2+}$•syt1 must penetrate, and bend, the target membrane to facilitate fusion[19,28,29]. Because $Ca^{2+}$ and membrane-bending are also involved in endocytosis[13,14,30,31], we sought to determine whether interactions between syt1 and $Ca^{2+}$/membranes are important for syt1-mediated acceleration of SV endocytosis.

We made use of previously reported mutations that alter the membrane penetration (and thereby membrane bending) and/or $Ca^{2+}$ binding activity of syt1[19,28]. In the first $Ca^{2+}$ ligand mutant form of syt1 that we examined, designated as $syt1^{4DN}$, two $Ca^{2+}$ ligands in C2A and two ligands in C2B were neutralized by substituting the native aspartatic acid residues with asparagines, such that syt1 cannot bind to $Ca^{2+}$ and is therefore unable to penetrate membranes. In the alanine mutant ($syt1^{4A}$), four non-polar residues within the membrane-penetration loops of C2A and C2B were replaced with alanines, such that the volume of the membrane penetration loops was reduced; these mutations virtually abolish the membrane penetration and bending activity of $Ca^{2+}$•$syt1^{19}$. Although the $Ca^{2+}$ binding activity of syt1 was attenuated by these mutations, vesicle co-flotation assays indicate that $syt1^{4A}$ can still bind to SNARE proteins to some extent in a $Ca^{2+}$-promoted manner[19], whereas $Ca^{2+}$-promoted SNARE binding activity was completely eliminated in $syt1^{4DN}$ [32]. When expressed in syt1 KO neurons, both of these syt1 mutants were present in presynaptic boutons (Supplementary Fig. 4). Nevertheless, $syt1^{4A}$ and $syt1^{4DN}$ both failed to rescue fast vesicle exocytosis (Fig. 3a, b; 793 ± 60 pA for $syt1^{FL}$; 107 ± 27 pA for $syt1^{4A}$, 83 ± 14 pA for $syt1^{4DN}$, $p<0.001$).

In contrast to the alanine mutant, we also increased the volume of the membrane penetration loops by substituting the same non-polar residues with tryptophans ($syt1^{4W}$); these mutations enhance the $Ca^{2+}$ dependent phospholipid binding - and membrane bending - activity of syt1[19,28,33]. When expressed in syt1 KO neurons, $syt1^{4W}$ was targeted to presynaptic boutons (Supplementary Fig. 4) where it mediated larger EPSCs as compared to $syt1^{FL}$ (1460 ± 130 pA, $p<0.001$). This increase was caused by higher SV release probability, since $syt1^{4W}$ resulted in a faster depletion of the SV pool during a 2 s 10 Hz stimulus train (Fig. 3c, d) [33].

Next, we evaluated the performance of all three syt1 point mutants during SV endocytosis using sypHy (Fig. 3e). The slow endocytosis observed in syt1 KO neurons was completely rescued by $syt1^{4A}$ or $syt1^{4W}$ (Fig. 3f, g; $\tau$: 21.9 ± 0.6 s for $syt1^{FL}$, 23.2 ± 0.5 s for $syt1^{4A}$, 23.5 ± 0.6 s for $syt1^{4W}$, $p>0.05$, compared to $syt1^{FL}$). The similar time constants for the alanine and tryptophan mutants indicate that membrane penetration does not play a role in syt1 promoted endocytosis. Furthermore, enhancement of the $Ca^{2+}$/membrane binding

affinity in syt1$^{4W}$ did not further accelerate endocytosis, consistent with our observations that increasing the extracellular [$Ca^{2+}$] from 1 to 3.5 mM does not accelerate the kinetics of endocytosis (Supplementary Fig. 5); physiological extracellular [$Ca^{2+}$] appears to be saturating under these conditions. In marked contrast to the syt1$^{4A}$ and syt1$^{4W}$ mutants, syt1$^{4DN}$ did not rescue slow endocytosis in syt1 KO neurons (Fig 3f, g; $\tau$: 33.1 ± 1.1 s; $p>0.05$, compared to syt1 KO). This observation was confirmed via FM4-64 uptake experiments (Supplementary Fig. 6).

We reiterate that membrane penetration loop mutations in syt1 either reduced (syt1$^{4A}$) or enhanced (syt1$^{4W}$) the function of syt1 during exocytosis without any secondary effects on the function of syt1 during endocytosis. Analogous to the retargeting experiments described above, these mutations clearly uncouple the role of syt1 in endo- and exocytosis. More importantly, both syt1$^{4A}$ and syt1$^{4DN}$ failed to rescue rapid exocytosis, but syt1$^{4A}$ did rescue normal rates of endocytosis in syt1 KO neurons. This difference between syt1$^{4A}$ and syt1$^{4DN}$ during vesicle retrieval can be attributed to the lack of $Ca^{2+}$ binding activity in syt1$^{4DN}$, but not to reductions in exocytosis. Together, these results strongly suggest that syt1 functions as a $Ca^{2+}$ sensor during SV endocytosis.

## $Ca^{2+}$ independent SV endocytosis does not rely upon syt1

The experiments reported thus far indicate that syt1 functions to accelerate $Ca^{2+}$-promoted endocytosis, but does syt1 also regulate $Ca^{2+}$-independent vesicle retrieval? To address this question, 20 Hz field stimulation was replaced with a 5 s superfusion of a hypertonic sucrose solution (0.5 M), to induce $Ca^{2+}$ independent exo-and endocytosis (Fig. 4a, Supplementary Fig. 8). Interestingly, endocytosis following sucrose treatment occurred with similar kinetics in WT and syt1 KO neurons (Fig. 4b, c) ($\tau$ of WT neurons: 17.0 ± 0.5 s for train stimulation, 15.5 ± 0.4 s for sucrose, $p>0.05$) ($\tau$ of syt1 KO neurons: 27.8 ± 0.9 s for train stimulation, 16.0 ± 0.4 s for sucrose, $p<0.001$), indicating that syt1 specifically functions during $Ca^{2+}$-regulated SV retrieval. We confirmed that the sucrose-induced changes in sypHy fluorescence intensity reflect changes in SV retrieval and are not due to mechanical effects (Supplementary Fig. 7).

## Both C2 domains can act as $Ca^{2+}$ sensors for SV endocytosis

The C2B domain of syt1 was originally proposed to be critical for endocytosis, because only this domain was found to bind AP-2[3,34]. However, recent studies suggested that syt1 interacts with stonin-2 through either C2 domain[7,35]. Here, we sought to determine which C2-domain of syt1 must sense $Ca^{2+}$ in order to accelerate endocytosis, by mutating two $Ca^{2+}$-ligands in either C2A (C2A$^{2DN}$-C2B) or C2B (C2A-C2B$^{2DN}$) (Fig. 5a), expressing these constructs in syt1 KO neurons, and conducting pHluorin imaging experiments. To avoid possible contributions of syt1 “null SVs” - which would, in effect, decelerate endocytosis - we tagged pHluorin directly to the luminal tail of the syt1 constructs used for these experiments. We note that the rate of endocytosis was identical in syt1 KO neurons expressing pH-syt1, as compared to WT neurons expressing sypHy (Supplementary Fig. 9).

Similar to syt1$^{4DN}$, which was characterized above, pH-syt1$^{4DN}$ was also unable to rescue rapid endocytosis (Fig. 5b, c; $\tau$: 39.3 ± 1.1 s for pH-syt1$^{4A}$, 17.5 ± 0.6 s for pH-syt1$^{FL}$,

p<0.001). Surprisingly, both C2A$^{2DN}$-C2B (16.1 ± 1.0 s) and C2A-C2B$^{2DN}$ (17.5 ± 0.5 s) exhibited normal rates of endocytosis (p>0.05), and the C2-domains appear to be completely redundant at this level of analysis. To further verify these findings, we investigated the performance of the $Ca^{2+}$-ligand mutants based on a 'scrambled' form of pH-syt1$^{FL}$, in which the order of C2A and C2B was exchanged in the primary sequence of the protein (C2B-C2A; Fig. 5a). Both C2B$^{2DN}$-C2A (17.5 ± 0.6 s), as well as C2B-C2A$^{2DN}$ (19.5 ± 0.6 s), restored normal rates of endocytosis in syt1 KO neurons (Fig. 5b, c; p>0.05, compared to pH-syt1$^{FL}$). We reiterate that $Ca^{2+}$-ligand mutations in the C2B domain disrupt the function of syt1 during exocytosis while analogous mutations in C2A do not[1,12,36,37]. Here, in sharp contrast to the function of syt1 in exocytosis, our data suggest that endocytosis can employ either C2-domain of syt1 to sense $Ca^{2+}$.

### C2A can internalize syt1 onto newly retrieved SVs

Given the surprising finding that C2A is capable of facilitating endocytosis by sensing $Ca^{2+}$, as indicated above, we next determined whether C2A alone can mediate the internalization of syt1. We generated two deletion mutants of syt1 that contained only one of the two C2-domains. These proteins were tagged with pHluorin on their N-terminal luminal domain (Fig. 6a) (pH-syt1$^{C2A}$, pH-syt1$^{C2B}$), to allow specific monitoring of the recycling of only those vesicles that harbored the mutant syt1 proteins.

We first examined the targeting efficiency of pH-syt1$^{C2A}$ and pH-syt1$^{C2B}$ (Fig. 6b), and found that they were only partially co-localized with synapsin I in presynaptic boutons (pH-syt1$^{C2A}$: 23 ± 2%; pH-syt1$^{C2B}$: 29 ± 2%), as compared to pH-syt1$^{FL}$ (71 ± 3%) (Fig. 6c). While the majority of boutons were devoid of the truncated mutant proteins, those boutons that contained the proteins showed robust immunofluorescence that was qualitatively similar to the signals obtained using full-length syt1-pH.

We next investigated the recycling kinetics of pH-syt1$^{C2A}$ and pH-syt1$^{C2B}$, and observed that pH-syt1$^{C2B}$ was able to facilitate endocytosis as effectively as pH-syt1$^{FL}$ (Fig. 6d, e; τ: 21.5 ± 0.9 s for pH-syt1$^{C2B}$, 18.8 ± 0.8 s for pH-syt1$^{FL}$, p>0.05). Surprisingly, expression of pH-syt1$^{C2A}$ resulted in efficient activity dependent de-quenching and re-quenching of pHluorin fluorescence, demonstrating that syt1 - lacking its C2B domain -can internalize into newly retrieved SVs (Fig. 6d, e; τ: 20.0 ± 0.9 s for pH-syt1$^{C2A}$). Although the C2A domain is unable to trigger fast vesicle exocytosis, this domain can sense $Ca^{2+}$ to facilitate SV endocytosis. These are the first data to directly support a role for C2A during SV endocytosis in neurons.

## DISCUSSION

It has been argued that perturbations that reduce exocytosis can indirectly affect endocytosis by reducing 'endocytic drive'[14], and thus far this trend has applied to all previous studies (e.g. see [8–10]). Hence, it remained unclear as to whether alterations in endocytosis, due to disruption of syt1, were secondary to defects in exocytosis. Here, we discovered that the function of syt1 in SV endocytosis is independent of its role in exocytosis, as evidenced by our uncoupling experiments (Fig. 1, 2). This observation made it possible to interpret a series of experiments in which the $Ca^{2+}$-binding activity of syt1 was abolished, revealing

that syt1 functions as a $Ca^{2+}$ sensor during SV endocytosis (Fig. 3, 4). This $Ca^{2+}$-sensor function is distinct from syt1's role in exocytosis, as both the C2A and C2B domains of syt1 are capable of sensing $Ca^{2+}$ to accelerate internalization of SVs (Fig. 5, 6), whereas only the C2B domain appears to be essential for exocytosis[36–38]. Together, these findings indicate that syt1 plays a role in coupling $Ca^{2+}$ regulated exo- and endocytosis in hippocampal neurons.

## Uncoupling the function of syt1 in SV exo- and endocytosis

In previous studies, defects in endocytosis induced by mutations or complete loss of syt1 were always associated with defects in exocytosis[8–10]. In a seminal study using acute photoinactivation of syt1[9,39], exocytosis was allowed to proceed in *shibire$^{ts}$* mutants at the restrictive temperature, then photoinactivation was carried out, and endocytosis was subsequently monitored at the permissive temperature and found to be absent. Recovery of endocytosis was not observed over the time frame of this experiment, and since syt1 is not required for endocytosis *per se*, these findings raise the possibility that the photoinactivated syt1 adduct actively inhibits endocytosis that would normally occur.

Uncoupling the roles of syt1 in endo- and exocytosis would greatly facilitate our understanding of the contribution of this molecule to the vesicle retrieval pathway. Here, we first addressed this problem by altering the local distribution of syt1 in neurons. Retargeting the cytoplasmic domain of syt1 to the plasma membrane uncoupled its roles in of exo- and endoctosis. In a second approach, we utilized point mutations to selectively alter exocytosis. For example, abolishing the membrane penetration activity of syt1 (syt1$^{4A}$) largely abolished exocytosis while leaving the ability of syt1 to facilitate endocytosis intact. This experiment revealed that changes in exocytosis do not always result in changes in endocytosis, at least in mouse hippocampal neurons; this result significantly impacts interpretation of the $Ca^{2+}$-ligand mutants, as detailed further below. Third, analysis of deletion mutants demonstrated that the C2A domain alone cannot trigger exocytosis but can sense $Ca^{2+}$ to facilitate rapid endocytosis.

Together, all three sets of experiments demonstrate that syt1 has a direct function in endocytosis, independent of its function in exocytosis.

## Syt1 as a dual $Ca^{2+}$ sensor for SV endo- and exocytosis

While both syt1$^{4A}$ and syt1$^{4W}$ were able to mediate rapid efficient endocytosis, syt1$^{4DN}$ failed to rescue normal endocytosis in syt1 KO neurons. Since syt1$^{4A}$ retains $Ca^{2+}$-sensing activity while syt1$^{4DN}$ is unable to bind $Ca^{2+}$, these results strongly suggest that syt1 must bind $Ca^{2+}$ in order to accelerate endocytosis. We further demonstrate that in hippocampal neurons, both the C2A and C2B domains of syt1 are capable of rescuing defects in endocytosis through binding to $Ca^{2+}$. Our results differ from a previous study carried out using *Drosophila*, in which a truncation mutant lacking C2B - but containing an intact C2A domain - could not rescue defects in endocytosis measured using a synaptobrevin-based pHluorin[11]. This apparent discrepancy might be due to inefficient targeting of truncated syt1 (Fig. 6b, c); a large number of synapses, devoid of mutant syt1, are likely to express the synaptobrevin-based optical reporter. To mitigate this concern, we fused a pHluorin directly

to syt1. By fusing the pH sensor directly to WT or truncated syt1 proteins, changes in fluorescence exclusively represent the recycling of SVs that harbor the mutant protein. Using this approach, we report for the first time that either C2A or C2B is able to accelerate endocytosis in neurons. However, in the *Drosophila* neuromuscular junction (NMJ), $Ca^{2+}$-ligand mutations in C2B alone disrupted endocytosis[11] and thus it appears that fly and mouse syt1 operate in distinct ways during vesicle retrieval.

We note that the study by Poskanzer et al. (2006) has been used as evidence for the idea that the decelerated endocytosis observed in syt1 deficient neurons was secondary to reduced rates of exocytosis[14]. However, this idea does not appear to apply to the system used in our studies, since we have shown that mutations in syt1 that reduce exocytosis do not always give rise to changes in the rate of endocytosis. If this is also true at the *Drosophila* NMJ, the C2B $Ca^{2+}$-ligand studies reported by Poskanzer et al. (2006) also support the notion that syt1 acts as a $Ca^{2+}$ sensor for SV endocytosis.

Our results regarding syt1 deletion mutants, that lacked either C2A or C2B, indicate that either C2-domain can accelerate endocytosis. The notion that the C2A domain participates in vesicle retrieval is novel and might be viewed as surprising since this domain cannot directly bind to AP-2μ[3,35]. However, as alluded to above, stonin-2, a sorting protein adaptor specific for syt1, is now believed to bind to C2A even more strongly than to C2B[35]. Thus the internalization of C2A is likely to involve the recruitment of stonin-2, as suggested by recent studies using non-neuronal cells[35].

## $Ca^{2+}$ sensors and modes of endocytosis

SV endocytosis occurs on time scales that are much slower than for exocytosis. Since kinetic studies demonstrate that syt1 binds and unbinds $Ca^{2+}$ and membranes in milliseconds[40], the question arises as to how syt1 can regulate endocytosis seconds after $Ca^{2+}$ microdomains have collapsed. One possible explanation is that syt1 interacts with an endocytic partner protein that gives rise to long-lived tripartite complexes with $Ca^{2+}$. While $Ca^{2+}$ might be retained in such complexes, it is also possible that $Ca^{2+}$ serves a permissive role to allow complex assembly but is not needed once complexes have formed. Alternatively, a regulatory protein might be bound to syt1 under resting conditions, but is released once syt1 binds $Ca^{2+}$, thereby allowing syt1 to accelerate endocytosis.

In WT neurons, we found that endocytosis - following application of hypertonic sucrose - was as rapid as the endocytosis that occurs following 20 Hz electrical stimulation (Fig. 4). Using sucrose, the rate of vesicle retrieval was not affected by loss of syt1. It is interesting that this $Ca^{2+}$-independent mode of endocytosis exhibits the same kinetics as the $Ca^{2+}$-dependent pathway. However, these two vesicle retrieval pathways are likely to involve different mechanisms; syt1 appears to play a role only in the $Ca^{2+}$-triggered pathway.

In different cell types, $Ca^{2+}$-dependent endocytosis might be mediated by distinct proteins. In addition to syt1, candidate $Ca^{2+}$ sensors include calcineurin[41–43] and calmodulin[14,44,45]. Calcineurin can promote endocytosis in cortical synaptosomes[41], but exerts an inhibitory effect during endocytosis at the *Drosophila* NMJ[46]. Recently, calcineurin was suggested to be crucial for activity dependent bulk endocytosis[43]. Calmodulin has been suggested to

operate as a $Ca^{2+}$ sensor for endocytosis in chromaffin cells[44,45] and the calyx of Held[14]. So, in hippocampal neurons, additional $Ca^{2+}$ sensors may serve to regulate endocytosis, analogous to the "two $Ca^{2+}$ sensor" model was proposed to explain the different temporal phases of neurotransmitter release[1,20,47].

## METHODS

### cDNA constructs

cDNA encoding sypHy (with two copies of a pH-sensitive GFP)[24,48] was kindly provided by E. Kavalali (Houston, TX) with permission from Y. Zhu (San Francisco, CA). cDNA for pH-syt1 was kindly provided by T. Ryan (New York, NY)[49]. For electrophysiology and fluorescence imaging experiments, a bicistronic lentiviral vector system, pLox Syn-DsRed-Syn-GFP (pLox) (kindly provided by F. Gomez-Scholl (Seville, Spain)) was used by substituting the DsRed coding sequence with the target cDNA sequence. One synapsin promoter (Syn) directs the expression of GFP while the other drives expression of the indicated syt1 construct. GFP serves as an in-vector marker to identify infected neurons. For pHluorin fluorescence imaging experiments, the GFP sequence in the pLox vector was substituted with mCherry to avoid spectral overlap with pHluorin. For experiments using fragments of syt1, the intact cytoplasmic domain of syt1 comprises residues 96 – 421, C2A consists of residues 96 – 265, and C2B comprises residues 248 – 421. For experiments using site mutant versions of syt1, Met 173, Phe 234, Val 304 and Ile 367 were mutated to Ala for $syt1^{4A}$, and to Trp for $syt1^{4W}$; Asp $Ca^{2+}$ ligands 230, 232 (in C2A), 363, and 365 (in C2B) were mutated to Asn for $syt1^{4DN}$. We also characterized syt1 mutants that harbored the $Ca^{2+}$-ligand mutations in only C2A (D230, 232N) or C2B (D363, 365N). To build the pH-syt10 construct used for experiments in Supplementary Fig. 7, we substituted full length syt10 for the full syt1 sequence in the pH-$syt1^{FL}$ construct[49].

### Cell culture and lentiviral infection

Cultured hippocampal neurons and chromaffin cells were prepared from postnatal day 0–1 mice as described previously[22]. Lentiviral particles were generated as described previously[19]. Neurons were infected with virus at 5 days *in vitro* (DIV) and analyzed at 16–21 DIV. Chromaffin cells were infected at 0 DIV and analyzed at 4 DIV.

### Electrophysiology

Whole-cell recordings were performed in voltage-clamp mode using a MultiClamp 700B amplifier (Molecular Devices). The recording chamber was continuously perfused with a bath solution (128 mM NaCl, 30 mM glucose, 5 mM KCl, 5 mM $CaCl_2$, 1 mM $MgCl_2$, 25 mM HEPES; pH 7.3) at room temperature. 50 μM D-AP5 (NMDA receptor antagonist; Tocris) and 20 μM bicuculline ($GABA_A$ receptor antagonist; Tocris) were applied to isolate AMPA receptor-mediated EPSCs. Patch pipettes were pulled from borosilicate glass and had resistances of 3–5 MΩ when filled with internal pipette solution (130 mM K-gluconate,1 mM EGTA, 5 mM Na-phosphocreatine, 2 mM Mg-ATP, 0.3 mM Na-GTP, 10 mM HEPES; pH 7.3). The series resistance was typically <15 MΩ and was partially compensated to 60–80%. The membrane potential was held at −70 mV. To trigger an action potential, presynaptic neurons were depolarized with a theta stimulating electrode, with a voltage step

from 0 V to 20–30 V for 1 millisecond; EPSCs were recorded from connected post-synaptic neurons. For mEPSC recording in Supplementary Fig. 2, the bath solution was supplemented with 0.5 μM tetrodotoxin (TTX) to block $Na^+$ channels. Data were acquired using pClamp software (Molecular Devices), sampled at 10 kHz, and filtered at 2 kHz. Off-line data analysis of EPSCs was performed using Clampfit and Igor (WaveMetrics) software.

## Fluorescence imaging

Neurons were continuously perfused with bath solution (in mM: 140 NaCl, 5 KCl, 2 $CaCl_2$, 2 $MgCl_2$, 10 HEPES, 10 glucose; in μM: 10 CNQX, 50 AP-5; pH 7.4). When $Ca^{2+}$ free bath solution was used, 2 mM $CaCl_2$ was replaced with 2 mM $MgCl_2$. Neurons were depolarized using 1 ms, 70 V, bipolar pulses via two parallel platinum wires embedded in the imaging chamber, or were superfused with hypertonic sucrose solution. For the AM-BAPTA experiments in Supplementary Fig. 8, neurons were perfused with $Ca^{2+}$ free bath solution containing 30 μM AM-BAPTA, and were pre-incubated with AM-BAPTA for 15 min prior to imaging experiments. A Xenon arc lamp was used as the light source for excitation, and images were acquired at 1 s intervals with a typical exposure time of 400 ms for pHluorin or 100 ms for FM4-64 on a Nikon TE300 inverted microscope. The following band pass optical filters (± 15~20 nm) were used: pHluorin (Excitation 484 nm, Emission 517 nm), FM4-64 (Ex 484 nm, Em 645 nm). A neutral density filter (ND 0.3, Chroma) was used for FM4-64 to minimize photobleaching. Fluorescence changes at individual boutons were monitored using an EMCCD camera (Cascade 512IIB, PhotoMetrics) with 2 × 2 binning, collected and analyzed off-line using MetaMorph software (Universal Imaging). In all experiments, images were acquired for 10 s prior to stimulation to establish a stable baseline. The regions that showed ΔF larger than 5 A.U. during stimulation were initially selected and marked with a 7-pixel diameter circle (corresponding to ~1.5 μm). This cut-off for selection (5 A.U.), which corresponds to 1.5 times the full-width half maximum of the Gaussian distribution of fluorescence noise, was determined as described previously [50]. Those regions that showed abrupt ΔF larger than 5 A.U. over any 3 consecutive time-points during the baseline acquisition were discarded. Further selection was based on morphology (oval shape) and immobility during acquisition. Bleaching was less than 1% for 120 s ~ 180 s time-lapse experiments and was not corrected.

## Antibodies and Immunocytochemistry

Mouse monoclonal antibodies specific for syt1 (41.1), NMDAR (54.1) or synaptophysin (7.2) used for immunoblot analysis were kindly provided by R. Jahn (Gottingen, Germany). The same antibody for syt1 (1:400), a chick polyclonal antibody specific for GFP (1:1000, Abcam), and a rabbit polyclonal antibody specific for synapsin I (1:200, Chemicon) were used to localize GAP43-C2AB and syt1 mutants. Cy3-conjugated anti-mouse (Jackson ImmunoResearch Laboratories) and Alexa647-conjugated anti-rabbit (Invitrogen) secondary antibodies (1:500) were used to visualize immunofluorescence. Immunocytochemistry was carried out and analyzed as described previously[22]. All images were collected using a Confocal microscope (FV1000; Olympus) with a 60X NA 1.10 water immersion objective (Olympus). Images were acquired using Fluoview software version 1.6 (Olympus), and analyzed using ImageJ (NIH) or Adobe Photoshop software (Adobe).

### Cell fractionation and Immunoblot analysis

Neurons were homogenized with a Dounce tissue grinder and centrifuged at 1k × g for 10 min to remove unbroken cells and large fragments. A crude synaptosomal pellet was collected after further high speed centrifugation at 12k × g for 15 min. The synaptosomal pellet was resuspended in HEPES buffer supplemented with 1 volume of 320 mM sucrose and lysed with 9 volumes of ice-cold water, followed by centrifugation at 66K × g for 25 minutes. The supernatant was collected and mixed with equal volumes of Optiprep solution and layered with 30% and 0% Optiprep. The step gradient was centrifuged at 20K × g for 5 hours and SVs were collected from the 0 ~ 30% interface. The protein concentration was determined using the BCA assay and 1 μg of each sample was resolved by SDS-PAGE. The samples were transferred to nitrocellulose and immunoblotted for SV and plasma membrane markers.

### Statistical analysis

The two-tailed unpaired Student's *t*-test was used to determine the statistical significance of observed differences between various conditions.

## Supplementary Material

Refer to Web version on PubMed Central for supplementary material.

## Acknowledgments

We thank E. Hui for providing constructs used for the electrophysiology experiments in Fig. 3. We also thank M.B. Jackson, X. Lou, and the Chapman lab for their comments on this manuscript. This study was supported by a grant from the National Institutes of Health (MH 61876). J.Y. is supported by an American Heart Association postdoctoral fellowship (11POST5720016). S.E.K was supported by an Epilepsy Foundation predoctoral fellowship. E.R.C. is an Investigator of the Howard Hughes Medical Institute.

## References

1. Koh TW, Bellen HJ. Synaptotagmin I, a $Ca^{2+}$ sensor for neurotransmitter release. Trend Neurosci. 2003; 26:413–422. [PubMed: 12900172]
2. Chapman ER. How Does Synaptotagmin Trigger Neurotransmitter Release? Annu Rev Biochem. 2008; 77:615–641. [PubMed: 18275379]
3. Zhang JZ, Davletov BA, Sudhof TC, Anderson RG. Synaptotagmin I is a high affinity receptor for clathrin AP-2: implications for membrane recycling. Cell. 1994; 78:751–760. [PubMed: 8087843]
4. Haucke V, Wenk MR, Chapman ER, Farsad K, De Camilli P. Dual interaction of synaptotagmin with μ2- and α-adaptin facilitates clathrin-coated pit nucleation. EMBO J. 2000; 19:6011–6019. [PubMed: 11080148]
5. Grass I, Thiel S, Honing S, Haucke V. Recognition of a basic AP-2 binding motif within the C2B domain of synaptotagmin is dependent on multimerization. J Biol Chem. 2004; 279:54872–54880. [PubMed: 15491995]
6. Walther K, Diril MK, Jung N, Haucke V. Functional dissection of the interactions of stonin 2 with the adaptor complex AP-2 and synaptotagmin. Proc Natl Acad Sci USA. 2004; 101:964–969. [PubMed: 14726597]
7. Diril MK, Wienisch M, Jung N, Klingauf J, Haucke V. Stonin 2 is an AP-2-dependent endocytic sorting adaptor for synaptotagmin internalization and recycling. Dev Cell. 2006; 10:233–244. [PubMed: 16459302]
8. Jorgensen EM, et al. Defective recycling of synaptic vesicles in synaptotagmin mutants of Caenorhabditis elegans. Nature. 1995; 378:196–199. [PubMed: 7477324]

9. Poskanzer KE, Marek KW, Sweeney ST, Davis GW. Synaptotagmin I is necessary for compensatory synaptic vesicle endocytosis in vivo. Nature. 2003; 426:559–563. [PubMed: 14634669]
10. Nicholson-Tomishima K, Ryan TA. Kinetic efficiency of endocytosis at mammalian CNS synapses requires synaptotagmin I. Proc Natl Acad Sci USA. 2004; 101:16648–16652. [PubMed: 15492212]
11. Poskanzer KE, Fetter RD, Davis GW. Discrete residues in the C2b domain of synaptotagmin I independently specify endocytic rate and synaptic vesicle size. Neuron. 2006; 50:49–62. [PubMed: 16600855]
12. Stevens CF, Sullivan JM. The synaptotagmin C2A domain is part of the calcium sensor controlling fast synaptic transmission. Neuron. 2003; 39:299–308. [PubMed: 12873386]
13. Hosoi N, Holt M, Sakaba T. Calcium dependence of exo- and endocytotic coupling at a glutamatergic synapse. Neuron. 2009; 63:216–229. [PubMed: 19640480]
14. Wu XS, et al. $Ca^{2+}$ and calmodulin initiate all forms of endocytosis during depolarization at a nerve terminal. Nat Neurosci. 2009; 12:1003–1010. [PubMed: 19633667]
15. Neale EA, Bowers LM, Jia M, Bateman KE, Williamson LC. Botulinum neurotoxin A blocks synaptic vesicle exocytosis but not endocytosis at the nerve terminal. J Cell Biol. 1999; 147:1249–1260. [PubMed: 10601338]
16. Neves G, Gomis A, Lagnado L. Calcium influx selects the fast mode of endocytosis in the synaptic terminal of retinal bipolar cells. Proc Natl Acad Sci USA. 2001; 98:15282–15287. [PubMed: 11734626]
17. Wu W, Xu J, Wu XS, Wu LG. Activity-dependent acceleration of endocytosis at a central synapse. J Neurosci. 2005; 25:11676–11683. [PubMed: 16354926]
18. Balaji J, Armbruster M, Ryan TA. Calcium control of endocytic capacity at a CNS synapse. J Neurosci. 2008; 28:6742–6749. [PubMed: 18579748]
19. Hui E, Johnson CP, Yao J, Dunning FM, Chapman ER. Synaptotagmin-mediated bending of the target membrane is a critical step in $Ca^{2+}$-regulated fusion. Cell. 2009; 138:709–721. [PubMed: 19703397]
20. Geppert M, et al. Synaptotagmin I: a major $Ca^{2+}$ sensor for transmitter release at a central synapse. Cell. 1994; 79:717–727. [PubMed: 7954835]
21. Nishiki T, Augustine GJ. Synaptotagmin I synchronizes transmitter release in mouse hippocampal neurons. J Neurosci. 2004; 24:6127–6132. [PubMed: 15240804]
22. Liu H, Dean C, Arthur CP, Dong M, Chapman ER. Autapses and networks of hippocampal neurons exhibit distinct synaptic transmission phenotypes in the absence of synaptotagmin I. J Neurosci. 2009; 29:7395–7403. [PubMed: 19515907]
23. Granseth B, Odermatt B, Royle SJ, Lagnado L. Clathrin-mediated endocytosis is the dominant mechanism of vesicle retrieval at hippocampal synapses. Neuron. 2006; 51:773–786. [PubMed: 16982422]
24. Zhu Y, Xu J, Heinemann SF. Two pathways of synaptic vesicle retrieval revealed by single-vesicle imaging. Neuron. 2009; 61:397–411. [PubMed: 19217377]
25. Miesenbock G, De Angelis DA, Rothman JE. Visualizing secretion and synaptic transmission with pH-sensitive green fluorescent proteins. Nature. 1998; 394:192–195. [PubMed: 9671304]
26. Fernandez-Alfonso T, Ryan TA. The kinetics of synaptic vesicle pool depletion at CNS synaptic terminals. Neuron. 2004; 41:943–953. [PubMed: 15046726]
27. Mani M, et al. The dual phosphatase activity of synaptojanin1 is required for both efficient synaptic vesicle endocytosis and reavailability at nerve terminals. Neuron. 2007; 56:1004–1018. [PubMed: 18093523]
28. Martens S, Kozlov MM, McMahon HT. How synaptotagmin promotes membrane fusion. Science. 2007; 316:1205–1208. [PubMed: 17478680]
29. Chicka MC, Hui E, Liu H, Chapman ER. Synaptotagmin arrests the SNARE complex before triggering fast, efficient membrane fusion in response to $Ca^{2+}$ Nat Struct Mol Biol. 2008; 15:827–835. [PubMed: 18622390]
30. Zhang B, Zelhof AC. Amphiphysins: raising the BAR for synaptic vesicle recycling and membrane dynamics. Traffic. 2002; 3:452–460. [PubMed: 12047553]

31. Schmidt A, et al. Endophilin I mediates synaptic vesicle formation by transfer of arachidonate to lysophosphatidic acid. Nature. 1999; 401:133–141. [PubMed: 10490020]
32. Earles CA, Bai J, Wang P, Chapman ER. The tandem C2 domains of synaptotagmin contain redundant $Ca^{2+}$ binding sites that cooperate to engage t-SNAREs and trigger exocytosis. J Cell Biol. 2001; 154:1117–1123. [PubMed: 11551981]
33. Rhee JS, et al. Augmenting neurotransmitter release by enhancing the apparent $Ca^{2+}$ affinity of synaptotagmin 1. Proc Natl Acad Sci USA. 2005; 102:18664–18669. [PubMed: 16352718]
34. Walther K, et al. Human stoned B interacts with AP-2 and synaptotagmin and facilitates clathrin-coated vesicle uncoating. EMBO Rep. 2001; 2:634–640. [PubMed: 11454741]
35. Jung N, et al. Molecular basis of synaptic vesicle cargo recognition by the endocytic sorting adaptor stonin 2. J Cell Biol. 2007; 179:1497–1510. [PubMed: 18166656]
36. Mackler JM, Drummond JA, Loewen CA, Robinson IM, Reist NE. The C(2)B $Ca^{2+}$-binding motif of synaptotagmin is required for synaptic transmission in vivo. Nature. 2002; 418:340–344. [PubMed: 12110842]
37. Nishiki T, Augustine GJ. Dual roles of the C2B domain of synaptotagmin I in synchronizing $Ca^{2+}$-dependent neurotransmitter release. J Neurosci. 2004; 24:8542–8550. [PubMed: 15456828]
38. Mackler JM, Reist NE. Mutations in the second C2 domain of synaptotagmin disrupt synaptic transmission at Drosophila neuromuscular junctions. J Comp Neurol. 2001; 436:4–16. [PubMed: 11413542]
39. Marek KW, Davis GW. Transgenically encoded protein photoinactivation (FlAsH-FALI): acute inactivation of synaptotagmin I. Neuron. 2002; 36:805–813. [PubMed: 12467585]
40. Hui E, et al. Three distinct kinetic groupings of the synaptotagmin family: candidate sensors for rapid and delayed exocytosis. Proc Natl Acad Sci USA. 2005; 102:5210–5214. [PubMed: 15793006]
41. Marks B, McMahon HT. Calcium triggers calcineurin-dependent synaptic vesicle recycling in mammalian nerve terminals. Curr Biol. 1998; 8:740–749. [PubMed: 9651678]
42. Cousin MA, Robinson PJ. The dephosphins: dephosphorylation by calcineurin triggers synaptic vesicle endocytosis. Trend Neurosci. 2001; 24:659–665. [PubMed: 11672811]
43. Clayton EL, Evans GJ, Cousin MA. Activity-dependent control of bulk endocytosis by protein dephosphorylation in central nerve terminals. J Physiol. 2007; 585:687–691. [PubMed: 17584836]
44. Artalejo CR, Henley JR, McNiven MA, Palfrey HC. Rapid endocytosis coupled to exocytosis in adrenal chromaffin cells involves $Ca^{2+}$, GTP, and dynamin but not clathrin. Proc Natl Acad Sci USA. 1995; 92:8328–8332. [PubMed: 7667289]
45. Artalejo CR, Elhamdani A, Palfrey HC. Calmodulin is the divalent cation receptor for rapid endocytosis, but not exocytosis, in adrenal chromaffin cells. Neuron. 1996; 16:195–205. [PubMed: 8562084]
46. Kuromi H, Yoshihara M, Kidokoro Y. An inhibitory role of calcineurin in endocytosis of synaptic vesicles at nerve terminals of Drosophila larvae. Neurosci Res. 1997; 27:101–113. [PubMed: 9100252]
47. Goda Y, Stevens CF. Two components of transmitter release at a central synapse. Proc Natl Acad Sci USA. 1994; 91:12942–12946. [PubMed: 7809151]
48. Atasoy D, et al. Spontaneous and evoked glutamate release activates two populations of NMDA receptors with limited overlap. J Neurosci. 2008; 28:10151–10166. [PubMed: 18829973]
49. Fernandez-Alfonso T, Kwan R, Ryan TA. Synaptic vesicles interchange their membrane proteins with a large surface reservoir during recycling. Neuron. 2006; 51:179–186. [PubMed: 16846853]
50. Richards DA, Bai J, Chapman ER. Two modes of exocytosis at hippocampal synapses revealed by rate of FM1-43 efflux from individual vesicles. J Cell Biol. 2005; 168:929–939. [PubMed: 15767463]

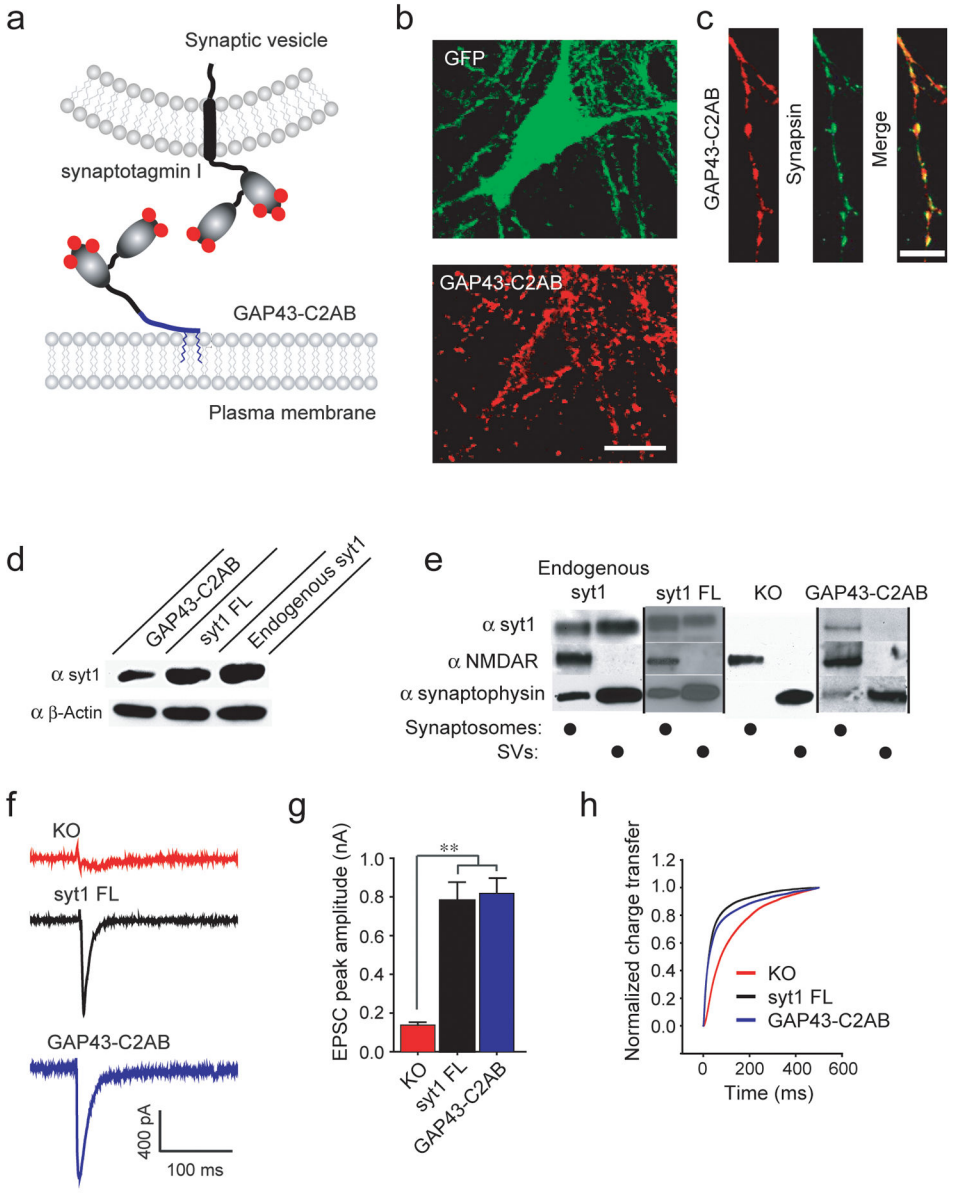


**Figure 1.**

Plasma membrane targeted cytoplasmic domain of syt1 rescues SV exocytosis in syt1 KO neurons. (a) Diagram of the GAP43-C2AB chimera. The cytoplasmic domain of syt1 (C2AB) was targeted to the presynaptic plasma membrane by fusing it to the first 20 residues of GAP-43. (b) Immunocytochemistry, using an anti-C2A domain antibody, indicated that GAP43-C2AB was localized to the plasma membrane while soluble GFP was cytosolic. Scale bar, 10 μm. (c) Immunostaining with an antibody specific for the C2A domain of syt1 showing that GAP43-C2AB was localized to synapsin I labeled presynaptic boutons. Scale bar, 4 μm. (d) Immunoblot analysis revealed that $syt1^{FL}$ was expressed in syt1 KO neurons at levels similar to endogenous syt1 in WTcells; GAP43-C2AB was expressed at somewhat lower levels (57 %). (e) Distribution of expressed syt1 constructs analyzed via subcellular fractionation of WT neurons, syt1 KO neurons, and KO neurons

expressing syt1$^{FL}$ or GAP43-C2AB. Antibodies directed against the NMDA receptor (NMDAR) or synaptophysin were used to distinguish plasma membrane from SV fractions, respectively. Vertical lines denote different blots. (f) Typical traces of evoked EPSCs recorded from syt1 KO neurons (KO) and lentivirus-infected KO neurons expressing syt1$^{FL}$ or GAP43-C2AB. (g) Bar graph showing the peak amplitude of EPSCs recorded from syt1 KO neurons (n = 24), KO neurons expressing syt1$^{FL}$ (n = 21) or GAP43-C2AB (n = 20). (h) Average normalized cumulative EPSC charge transfer over 0.5 s for KO neurons expressing the indicated constructs. ** $p<0.001$. Error bars represent SEM.

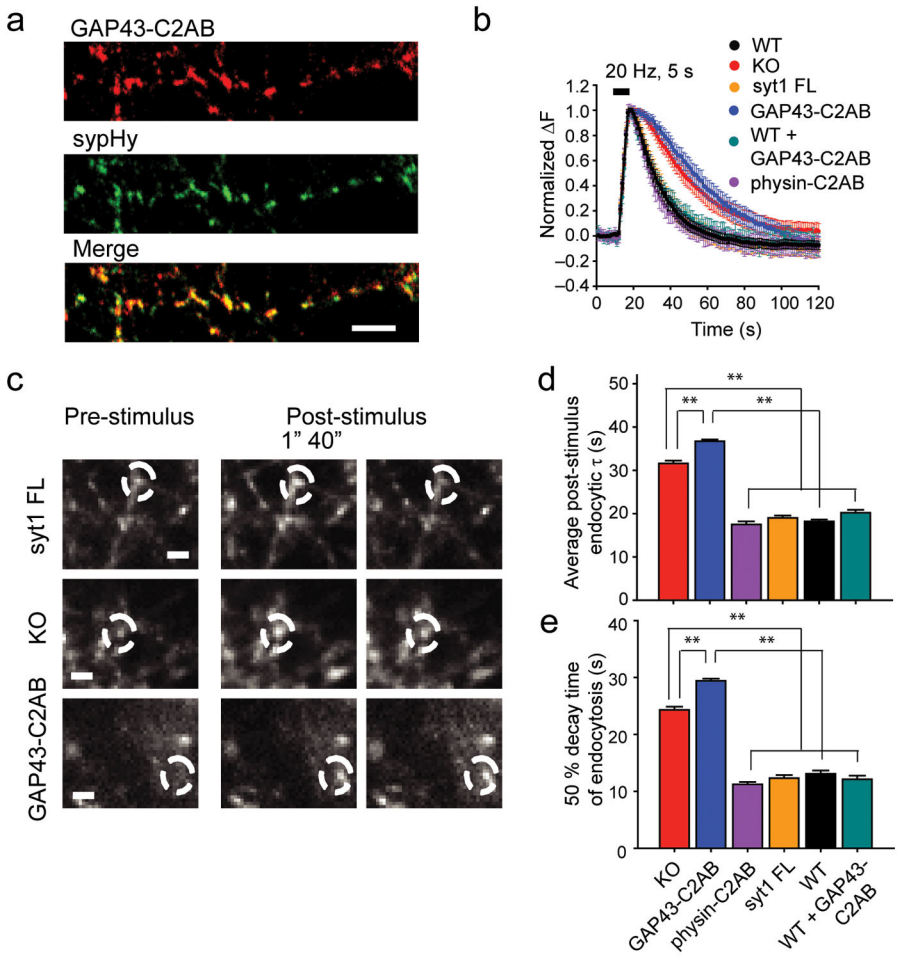


**Figure 2.**

GAP43-C2AB cannot rescue defective SV endocytosis in syt1 KO neurons. (a) Upper panel, immunostaining with an antibody specific for the C2A domain of syt1 (41.1) was used to visualize GAP43-C2AB. Middle panel, An antibody specific for pHluorin/GFP was used to visualize sypHy. Lower panel, merged image. Scale bar, 5 μm. (b) Normalized fluorescence changes of sypHy in WT neurons (n = 96), syt1 KO neurons (n = 120), and KO neurons expressing $syt1^{FL}$ (n = 100), GAP43-C2AB (n = 115), or physin-C2AB (n = 95), as well as WT neurons expressing GAP43-C2AB (n = 74). 'n' is total number of boutons pooled from 4 coverslips. (c) Sample images showing sypHy fluorescence in presynaptic boutons before, 1 s after, and 40 s after 100 stimuli at 20 Hz. Images were recorded from syt1 KO neurons and KO neurons expressing $syt1^{FL}$ or GAP43-C2AB. Scale bar, 2 μm. (d & e) Bar graph comparing the endocytic τ and 50% decay time. ** $p<0.001$. Error bars represent SEM.

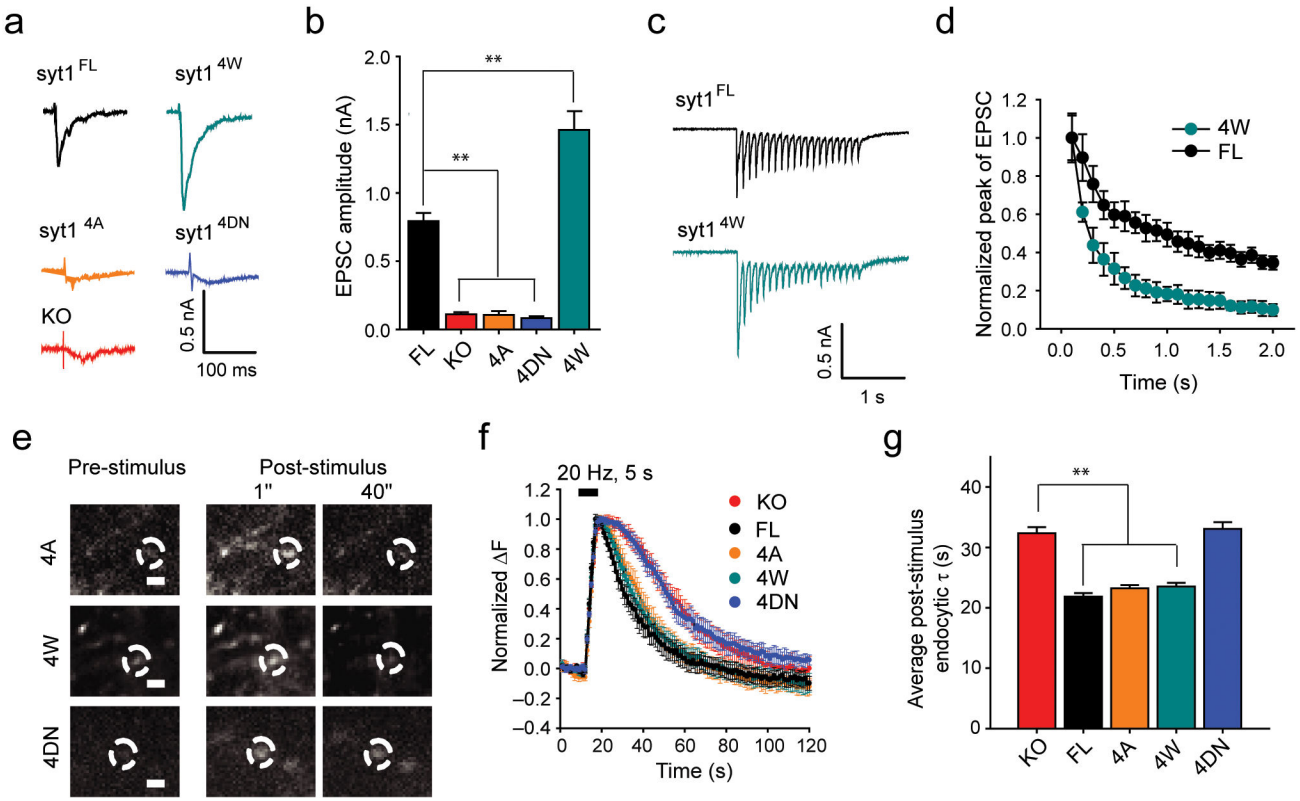


**Figure 3.**

$Ca^{2+}$ binding activity is required for syt1 to accelerate SV endocytosis. (a) Representative traces of EPSCs triggered by single action potentials. (b) Bar graph summarizing the peak amplitude of EPSCs recorded from syt1 KO neurons with lentiviral expression of $syt1^{FL}$ (n = 29), $syt1^{4A}$ (n = 15), $syt1^{4W}$ (n = 24) or $syt1^{4DN}$ (n = 17). (c) Representative traces showing EPSCs evoked by a 2 s 10 Hz stimulus train in syt1 KO neurons expressing $syt1^{FL}$ or $syt1^{4W}$. (d) Normalized peak amplitudes of EPSCs during 2 s 10 Hz train stimulation ($syt1^{FL}$, n = 14; $syt1^{4W}$, n = 13). (e) Sample images showing sypHy fluorescence in presynaptic boutons before, 1 s after and 40 s after 100 action potentials at 20 Hz. Images were acquired from syt1 KO neurons and KO neurons expressing $syt1^{4A}$, $syt1^{4W}$, or $syt1^{4DN}$. Scale bar, 2 μm. (f) Normalized fluorescence changes of sypHy in syt1 KO neurons (n = 95), and KO neurons expressing $syt1^{FL}$ (n = 102), $syt1^{4A}$ (n = 100), $syt1^{4W}$ (n = 110), or $syt1^{4DN}$ (n = 84). 'n' is total number of boutons pooled from 4–5 coverslips. (g) Bar graph summarizing the endocytic time constants of $syt1^{FL}$, $syt1^{4A}$, $syt1^{4W}$, or $syt1^{4DN}$. ** $p<0.001$. Error bars represent SEM.

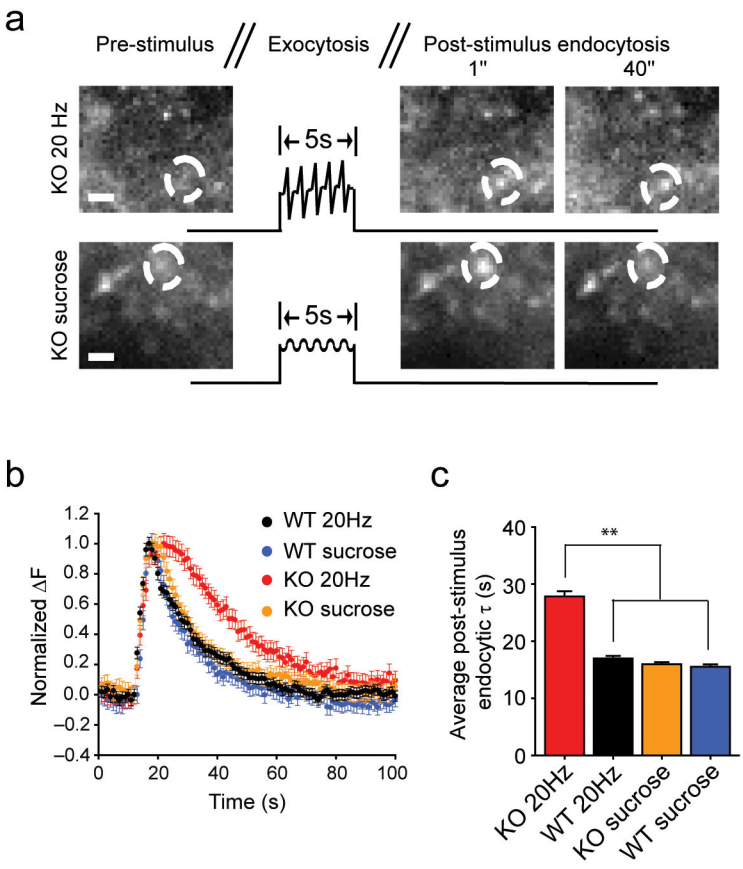


**Figure 4.**

$Ca^{2+}$ independent SV endocytosis does not rely upon syt1. (a) Experimental protocol and typical images showing exo- and endocytosis in syt1 KO neurons. Neurons were subjected to 5 s field-stimulation (20 Hz) or, for induction of $Ca^{2+}$ independent exocytosis and subsequent endocytosis, were superfused with a 0.5 M hypertonic sucrose solution for 5 s. Scale bar, 2 μm. (b) Normalized fluorescence changes of sypHy in WT neurons and syt1 KO neurons in response to train stimulation or sucrose superfusion. WT/sucrose, n = 79; WT/train, n = 137; KO/sucrose, n = 77; KO/train, n = 103. 'n' is total number of boutons pooled from 4–5 coverslips. (c) Bar graph summarizing the τ values for endocytosis in WT and syt1 KO neurons in response to train stimulation or sucrose superfusion. * $p<0.05$, ** $p<0.001$. Error bars represent SEM.

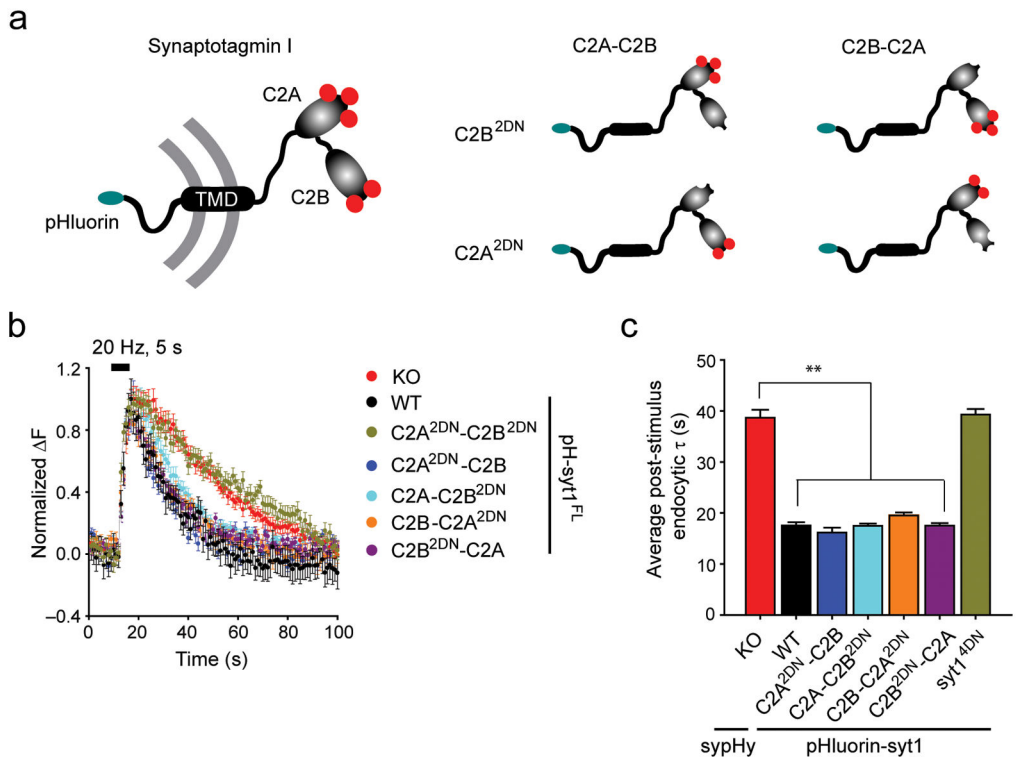


**Figure 5.**

C2A and C2B are redundant $Ca^{2+}$ sensors for endocytosis. (a) Diagram showing the $Ca^{2+}$ ligand mutant forms of pHluorin tagged syt1 employed for fluorescence imaging experiments. (b) Normalized fluorescence changes in syt1 KO neurons expressing sypHy (n = 52), pH-$syt1^{FL}$ (n = 64) or $Ca^{2+}$ ligand mutants of pH-$syt1^{FL}$ (pH-$syt1^{4DN}$, n = 48; $C2A^{2DN}$-C2B, n = 72; C2A-$C2B^{2DN}$, n = 61; $C2B^{2DN}$-C2A, n = 50; C2B-$C2A^{2DN}$, n = 60). 'n' is total number of boutons pooled from 4 coverslips. (c) Bar graph summarizing the τ values for endocytosis in (B). ** $p<0.001$. Error bars represent SEM.

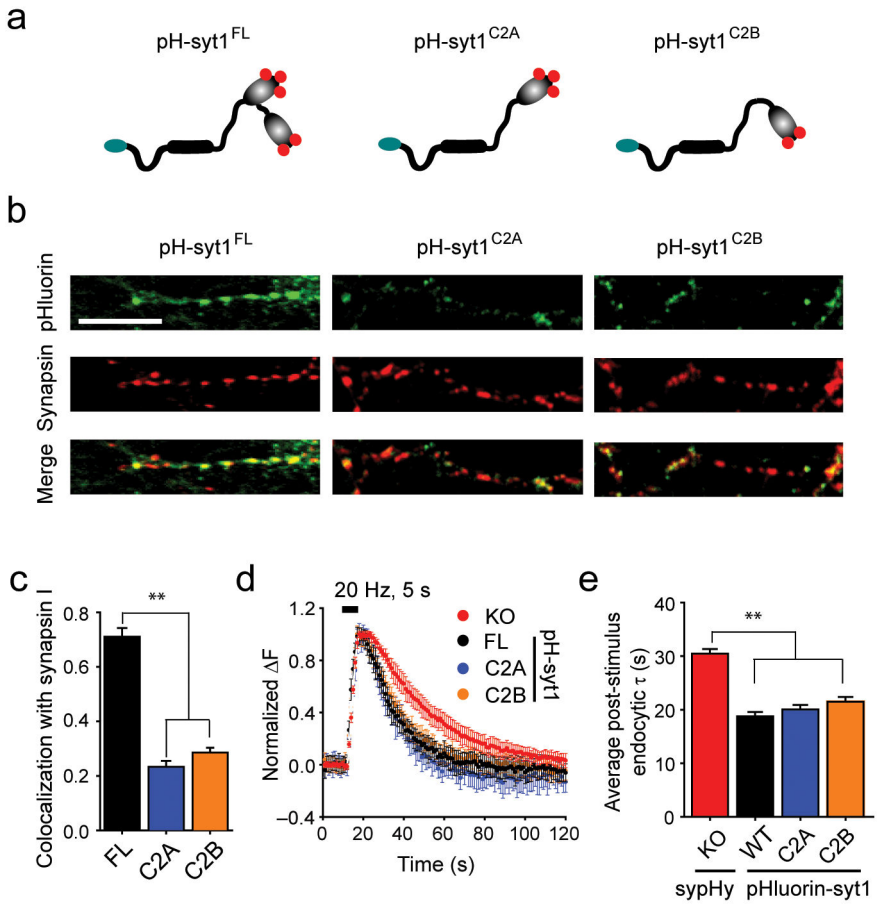


**Figure 6.**

The C2A domain is capable of internalizing syt1 into newly retrieved SVs. (a) Diagram showing the pHluorin tagged syt1 mutants, pH-syt1$^{C2A}$ and pH-syt1$^{C2B}$. (b) Immunostaining analysis revealed that small fractions of pH-syt1$^{C2A}$ and pH-syt1$^{C2B}$, as compared to pH-syt1$^{FL}$, were localized to presynaptic boutons. An antibody specific for pHluorin/GFP was used to visualize pH-syt1$^{C2A}$ and pH-syt1$^{C2B}$. An anti-synapsin I antibody was used to label presynaptic boutons. Scale bar, 5 μm. (c) Bar graph comparing the presence of pH-syt1$^{C2A}$ (n = 15) or pH-syt1$^{C2B}$ (n = 13) in presynaptic boutons labeled with a synapsin I antibody, as compared to pH-syt1$^{FL}$ (n = 8). (d) Normalized fluorescence changes in syt1 KO neurons expressing sypHy (n = 69), pH-syt1$^{FL}$ (n = 80), pH-syt1$^{C2A}$ (n = 60), or pH-syt1$^{C2B}$ (n = 78). ‘n’ is total number of boutons pooled from 4 coverslips. (e) Bar graph summarizing τ values for endocytosis for each construct. ** $p<0.001$. Error bars represent SEM.